Measurement of the Cabibbo-Kobayashi-Maskawa Matrix Element $|V_{ub}|$ with $B \to \rho e \nu$ Decays

B. Aubert,[1] R. Barate,[1] D. Boutigny,[1] J.-M. Gaillard,[1] A. Hicheur,[1] Y. Karyotakis,[1] J. P. Lees,[1] P. Robbe,[1] V. Tisserand,[1] A. Zghiche,[1] A. Palano,[2] A. Pompili,[2] J. C. Chen,[3] N. D. Qi,[3] G. Rong,[3] P. Wang,[3] Y. S. Zhu,[3] G. Eigen,[4] I. Ofte,[4] B. Stugu,[4] G. S. Abrams,[5] A.W. Borgland,[5] A. B. Breon,[5] D. N. Brown,[5] J. Button-Shafer,[5] R. N. Cahn,[5] E. Charles,[5] M. S. Gill,[5] A.V. Gritsan,[5] Y. Groysman,[5] R. G. Jacobsen,[5] R.W. Kadel,[5] J. Kadyk,[5] L.T. Kerth,[5] Yu. G. Kolomensky,[5] J. F. Kral,[5] C. LeClerc,[5] M. E. Levi,[5] G. Lynch,[5] L. M. Mir,[5] P. J. Oddone,[5] T. J. Orimoto,[5] M. Pripstein,[5] N. A. Roe,[5] A. Romosan,[5] M.T. Ronan,[5] V. G. Shelkov,[5] A.V. Telnov,[5] W. A. Wenzel,[5] T. J. Harrison,[6] C. M. Hawkes,[6] D. J. Knowles,[6] S.W. O'Neale,[6] R. C. Penny,[6] A. T. Watson,[6] N. K. Watson,[6] T. Deppermann,[7] K. Goetzen,[7] H. Koch,[7] B. Lewandowski,[7] M. Pelizaeus,[7] K. Peters,[7] H. Schmuecker,[7] M. Steinke,[7] N. R. Barlow,[8] W. Bhimji,[8] J.T. Boyd,[8] N. Chevalier,[8] P. J. Clark,[8] W. N. Cottingham,[8] C. Mackay,[8] F. F. Wilson,[8] C. Hearty,[9] T. S. Mattison,[9] J. A. McKenna,[9] D. Thiessen,[9] S. Jolly,[10] P. Kyberd,[10] A. K. McKemey,[10] V. E. Blinov,[11] A. D. Bukin,[11] A. R. Buzykaev,[11] V. B. Golubev,[11] V. N. Ivanchenko,[11] A. A. Korol,[11] E. A. Kravchenko,[11] A. P. Onuchin,[11] S. I. Serednyakov,[11] Yu. I. Skovpen,[11] A. N. Yushkov,[11] D. Best,[12] M. Chao,[12] D. Kirkby,[12] A. J. Lankford,[12] M. Mandelkern,[12] S. McMahon,[12] R. K. Mommsen,[12] D. P. Stoker,[12] C. Buchanan,[13] H. K. Hadavand,[14] E. J. Hill,[14] D. B. MacFarlane,[14] H. P. Paar,[14] Sh. Rahatlou,[14] G. Raven,[14] U. Schwanke,[14] V. Sharma,[14] J.W. Berryhill,[15] C. Campagnari,[15] B. Dahmes,[15] N. Kuznetsova,[15] S. L. Levy,[15] O. Long,[15] A. Lu,[15] M. A. Mazur,[15] J. D. Richman,[15] W. Verkerke,[15] J. Beringer,[16] A. M. Eisner,[16] M. Grothe,[16] C. A. Heusch,[16] W. S. Lockman,[16] T. Pulliam,[16] T. Schalk,[16] R. E. Schmitz,[16] B. A. Schumm,[16] A. Seiden,[16] M. Turri,[16] W. Walkowiak,[16] D. C. Williams,[16] M. G. Wilson,[16] J. Albert,[17] E. Chen,[17] G. P. Dubois-Felsmann,[17] A. Dvoretskii,[17] D. G. Hitlin,[17] I. Narsky,[17] F. C. Porter,[17] A. Ryd,[17] A. Samuel,[17] S. Yang,[17] S. Jayatilleke,[18] G. Mancinelli,[18] B. T. Meadows,[18] M. D. Sokoloff,[18] T. Barillari,[19] F. Blanc,[19] P. Bloom,[19] W. T. Ford,[19] U. Nauenberg,[19] A. Olivas,[19] P. Rankin,[19] J. Roy,[19] J. G. Smith,[19] W. C. van Hoek,[19] L. Zhang,[19] J. L. Harton,[20] T. Hu,[20] A. Soffer,[20] W. H. Toki,[20] R. J. Wilson,[20] J. Zhang,[20] D. Altenburg,[21] T. Brandt,[21] J. Brose,[21] T. Colberg,[21] M. Dickopp,[21] R. S. Dubitzky,[21] A. Hauke,[21] H. M. Lacker,[21] E. Maly,[21] R. Müller-Pfefferkorn,[21] R. Nogowski,[21] S. Otto,[21] K. R. Schubert,[21] R. Schwierz,[21] B. Spaan,[21] L. Wilden,[21] D. Bernard,[22] G. R. Bonneaud,[22] F. Brochard,[22] J. Cohen-Tanugi,[22] S. T'Jampens,[22] Ch. Thiebaux,[22] G. Vasileiadis,[22] M. Verderi,[22] A. Anjomshoaa,[23] R. Bernet,[23] A. Khan,[23] D. Lavin,[23] F. Muheim,[23] S. Playfer,[23] J. E. Swain,[23] J. Tinslay,[23] M. Falbo,[24] C. Borean,[25] C. Bozzi,[25] L. Piemontese,[25] A. Sarti,[25] E. Treadwell,[26] F. Anulli,[27,*] R. Baldini-Ferroli,[27] A. Calcaterra,[27] R. de Sangro,[27] D. Falciai,[27] G. Finocchiaro,[27] P. Patteri,[27] I. M. Peruzzi,[27,*] M. Piccolo,[27] A. Zallo,[27] S. Bagnasco,[28] A. Buzzo,[28] R. Contri,[28] G. Crosetti,[28] M. Lo Vetere,[28] M. Macri,[28] M. R. Monge,[28] S. Passaggio,[28] F. C. Pastore,[28] C. Patrignani,[28] E. Robutti,[28] A. Santroni,[28] S. Tosi,[28] S. Bailey,[29] M. Morii,[29] G. J. Grenier,[30] U. Mallik,[30] J. Cochran,[31] H. B. Crawley,[31] J. Lamsa,[31] W. T. Meyer,[31] S. Prell,[31] E. I. Rosenberg,[31] J. Yi,[31] M. Davier,[32] G. Grosdidier,[32] A. Höcker,[32] S. Laplace,[32] F. Le Diberder,[32] V. Lepeltier,[32] A. M. Lutz,[32] T. C. Petersen,[32] S. Plaszczynski,[32] M. H. Schune,[32] L. Tantot,[32] G. Wormser,[32] R. M. Bionta,[33] V. Brigljević,[33] D. J. Lange,[33] K. van Bibber,[33] D. M. Wright,[33] A. J. Bevan,[34] J. R. Fry,[34] E. Gabathuler,[34] R. Gamet,[34] M. George,[34] M. Kay,[34] D. J. Payne,[34] R. J. Sloane,[34] C. Touramanis,[34] M. L. Aspinwall,[35] D. A. Bowerman,[35] P. D. Dauncey,[35] U. Egede,[35] I. Eschrich,[35] G.W. Morton,[35] J. A. Nash,[35] P. Sanders,[35] G. P. Taylor,[35] J. J. Back,[36] G. Bellodi,[36] P. Dixon,[36] P. F. Harrison,[36] H.W. Shorthouse,[36] P. Strother,[36] P. B. Vidal,[36] G. Cowan,[37] H. U. Flaecher,[37] S. George,[37] M. G. Green,[37] A. Kurup,[37] C. E. Marker,[37] T. R. McMahon,[37] S. Ricciardi,[37] F. Salvatore,[37] G. Vaitsas,[37] M. A. Winter,[37] D. Brown,[38] C. L. Davis,[38] J. Allison,[39] R. J. Barlow,[39] A. C. Forti,[39] P. A. Hart,[39] F. Jackson,[39] G. D. Lafferty,[39] A. J. Lyon,[39] N. Savvas,[39] J. H. Weatherall,[39] J. C. Williams,[39] A. Farbin,[40] A. Jawahery,[40] V. Lillard,[40] D. A. Roberts,[40] G. Blaylock,[41] C. Dallapiccola,[41] K. T. Flood,[41] S. S. Hertzbach,[41] R. Kofler,[41] V. B. Koptchev,[41] T. B. Moore,[41] H. Staengle,[41] S. Willocq,[41] R. Cowan,[42] G. Sciolla,[42] F. Taylor,[42] R. K. Yamamoto,[42] M. Milek,[43] P. M. Patel,[43] F. Palombo,[44] J. M. Bauer,[45] L. Cremaldi,[45] V. Eschenburg,[45] R. Kroeger,[45] J. Reidy,[45] D. A. Sanders,[45] D. J. Summers,[45] H. Zhao,[45] C. Hast,[46] P. Taras,[46] H. Nicholson,[47] C. Cartaro,[48] N. Cavallo,[48] G. De Nardo,[48] F. Fabozzi,[48,†] C. Gatto,[48] L. Lista,[48] P. Paolucci,[48] D. Piccolo,[48] C. Sciacca,[48] J. M. LoSecco,[49] J. R. G. Alsmiller,[50] T. A. Gabriel,[50] B. Brau,[51] J. Brau,[52] R. Frey,[52] M. Iwasaki,[52] C. T. Potter,[52] N. B. Sinev,[52] D. Strom,[52] E. Torrence,[52] F. Colecchia,[53] A. Dorigo,[53] F. Galeazzi,[53] M. Margoni,[53] M. Morandin,[53] M. Posocco,[53] M. Rotondo,[53] F. Simonetto,[53] R. Stroili,[53] G. Tiozzo,[53] C. Voci,[53] M. Benayoun,[54] H. Briand,[54] J. Chauveau,[54] P. David,[54] Ch. de la Vaissière,[54] L. Del Buono,[54] O. Hamon,[54] Ph. Leruste,[54] J. Ocariz,[54] M. Pivk,[54] L. Roos,[54] J. Stark,[54] P. F. Manfredi,[55] V. Re,[55] V. Speziali,[55] L. Gladney,[56] Q. H. Guo,[56] J. Panetta,[56] C. Angelini,[57] G. Batignani,[57]

 0031-9007/03/90(18)/181801(7)$20.00

S. Bettarini,[57] M. Bondioli,[57] F. Bucci,[57] G. Calderini,[57] E. Campagna,[57] M. Carpinelli,[57] F. Forti,[57] M. A. Giorgi,[57] A. Lusiani,[57] G. Marchiori,[57] F. Martinez-Vidal,[57] M. Morganti,[57] N. Neri,[57] E. Paoloni,[57] M. Rama,[57] G. Rizzo,[57] F. Sandrelli,[57] G. Triggiani,[57] J. Walsh,[57] M. Haire,[58] D. Judd,[58] K. Paick,[58] L. Turnbull,[58] D. E. Wagoner,[58] N. Danielson,[59] P. Elmer,[59] C. Lu,[59] V. Miftakov,[59] J. Olsen,[59] A. J. S. Smith,[59] A. Tumanov,[59] E.W. Varnes,[59] F. Bellini,[60] G. Cavoto,[59,60] D. del Re,[60] R. Faccini,[14,60] F. Ferrarotto,[60] F. Ferroni,[60] M. Gaspero,[60] E. Leonardi,[60] M. A. Mazzoni,[60] S. Morganti,[60] G. Piredda,[60] F. Safai Tehrani,[60] M. Serra,[60] C. Voena,[60] S. Christ,[61] G. Wagner,[61] R. Waldi,[61] T. Adye,[62] N. De Groot,[62] B. Franek,[62] N. I. Geddes,[62] G. P. Gopal,[62] E. O. Olaiya,[62] S. M. Xella,[62] R. Aleksan,[63] S. Emery,[63] A. Gaidot,[63] P.-F. Giraud,[63] G. Hamel de Monchenault,[63] W. Kozanecki,[63] M. Langer,[63] G.W. London,[63] B. Mayer,[63] G. Schott,[63] B. Serfass,[63] G. Vasseur,[63] Ch. Yeche,[63] M. Zito,[63] M.V. Purohit,[64] A.W. Weidemann,[64] F. X. Yumiceva,[64] K. Abe,[65] D. Aston,[65] R. Bartoldus,[65] N. Berger,[65] A. M. Boyarski,[65] O. L. Buchmueller,[65] M. R. Convery,[65] D. P. Coupal,[65] D. Dong,[65] J. Dorfan,[65] W. Dunwoodie,[65] R. C. Field,[65] T. Glanzman,[65] S. J. Gowdy,[65] E. Grauges-Pous,[65] T. Hadig,[65] V. Halyo,[65] T. Himel,[65] T. Hryn'ova,[65] M. E. Huffer,[65] W. R. Innes,[65] C. P. Jessop,[65] M. H. Kelsey,[65] P. Kim,[65] M. L. Kocian,[65] U. Langenegger,[65] D.W. G. S. Leith,[65] S. Luitz,[65] V. Luth,[65] H. L. Lynch,[65] H. Marsiske,[65] S. Menke,[65] R. Messner,[65] D. R. Muller,[65] C. P. O'Grady,[65] V. E. Ozcan,[65] A. Perazzo,[65] M. Perl,[65] S. Petrak,[65] B. N. Ratcliff,[65] S. H. Robertson,[65] A. Roodman,[65] A. A. Salnikov,[65] T. Schietinger,[65] R. H. Schindler,[65] J. Schwiening,[65] G. Simi,[65] A. Snyder,[65] A. Soha,[65] J. Stelzer,[65] D. Su,[65] M. K. Sullivan,[65] H. A. Tanaka,[65] J. Va'vra,[65] S. R. Wagner,[65] M. Weaver,[65] A. J. R. Weinstein,[65] W. J. Wisniewski,[65] D. H. Wright,[65] C. C. Young,[65] P. R. Burchat,[66] C. H. Cheng,[66] T. I. Meyer,[66] C. Roat,[66] W. Bugg,[67] M. Krishnamurthy,[67] S. M. Spanier,[67] J. M. Izen,[68] I. Kitayama,[68] X. C. Lou,[68] F. Bianchi,[69] M. Bona,[69] D. Gamba,[69] L. Bosisio,[70] G. Della Ricca,[70] S. Dittongo,[70] L. Lanceri,[70] P. Poropat,[70] L. Vitale,[70] G. Vuagnin,[70] R. Henderson,[71] R. S. Panvini,[72] Sw. Banerjee,[73] C. M. Brown,[73] D. Fortin,[73] P. D. Jackson,[73] R. Kowalewski,[73] J. M. Roney,[73] H. R. Band,[74] S. Dasu,[74] M. Datta,[74] A. M. Eichenbaum,[74] H. Hu,[74] J. R. Johnson,[74] R. Liu,[74] F. Di Lodovico,[74] A. K. Mohapatra,[74] Y. Pan,[74] R. Prepost,[74] S. J. Sekula,[74] J. H. von Wimmersperg-Toeller,[74] J. Wu,[74] S. L. Wu,[74] Z. Yu,[74] and H. Neal[75]

(*BABAR* Collaboration)

[1]*Laboratoire de Physique des Particules, F-74941 Annecy-le-Vieux, France*
[2]*Dipartimento di Fisica and INFN, Università di Bari, I-70126 Bari, Italy*
[3]*Institute of High Energy Physics, Beijing 100039, China*
[4]*Institute of Physics, University of Bergen, N-5007 Bergen, Norway*
[5]*Lawrence Berkeley National Laboratory and University of California, Berkeley, California 94720, USA*
[6]*University of Birmingham, Birmingham B15 2TT, United Kingdom*
[7]*Institut für Experimentalphysik 1, Ruhr Universität Bochum, D-44780 Bochum, Germany*
[8]*University of Bristol, Bristol BS8 1TL, United Kingdom*
[9]*University of British Columbia, Vancouver, BC, Canada V6T 1Z1*
[10]*Brunel University, Uxbridge, Middlesex UB8 3PH, United Kingdom*
[11]*Budker Institute of Nuclear Physics, Novosibirsk 630090, Russia*
[12]*University of California at Irvine, Irvine, California 92697, USA*
[13]*University of California at Los Angeles, Los Angeles, California 90024, USA*
[14]*University of California at San Diego, La Jolla, California 92093, USA*
[15]*University of California at Santa Barbara, Santa Barbara, California 93106, USA*
[16]*Institute for Particle Physics, University of California at Santa Cruz, Santa Cruz, California 95064, USA*
[17]*California Institute of Technology, Pasadena, California 91125, USA*
[18]*University of Cincinnati, Cincinnati, Ohio 45221, USA*
[19]*University of Colorado, Boulder, Colorado 80309, USA*
[20]*Colorado State University, Fort Collins, Colorado 80523, USA*
[21]*Institut für Kern-und Teilchenphysik, Technische Universität Dresden, D-01062 Dresden, Germany*
[22]*Ecole Polytechnique, LLR, F-91128 Palaiseau, France*
[23]*University of Edinburgh, Edinburgh EH9 3JZ, United Kingdom*
[24]*Elon University, Elon University, North Carolina 27244-2010, USA*
[25]*Dipartimento di Fisica and INFN, Università di Ferrara, I-44100 Ferrara, Italy*
[26]*Florida A&M University, Tallahassee, Florida 32307, USA*
[27]*Laboratori Nazionali di Frascati dell'INFN, I-00044 Frascati, Italy*
[28]*Dipartimento di Fisica and INFN, Università di Genova, I-16146 Genova, Italy*
[29]*Harvard University, Cambridge, Massachusetts 02138, USA*
[30]*University of Iowa, Iowa City, Iowa 52242, USA*

[31]*Iowa State University, Ames, Iowa 50011-3160, USA*
[32]*Laboratoire de l'Accélérateur Linéaire, F-91898 Orsay, France*
[33]*Lawrence Livermore National Laboratory, Livermore, California 94550, USA*
[34]*University of Liverpool, Liverpool L69 3BX, United Kingdom*
[35]*Imperial College, University of London, London SW7 2BW, United Kingdom*
[36]*Queen Mary, University of London, E1 4NS, United Kingdom*
[37]*Royal Holloway and Bedford New College, University of London, Egham, Surrey TW20 0EX, United Kingdom*
[38]*University of Louisville, Louisville, Kentucky 40292, USA*
[39]*University of Manchester, Manchester M13 9PL, United Kingdom*
[40]*University of Maryland, College Park, Maryland 20742, USA*
[41]*University of Massachusetts, Amherst, Massachusetts 01003, USA*
[42]*Laboratory for Nuclear Science, Massachusetts Institute of Technology, Cambridge, Massachusetts 02139, USA*
[43]*McGill University, Montréal, QC, Canada H3A 2T8*
[44]*Dipartimento di Fisica and INFN, Università di Milano, I-20133 Milano, Italy*
[45]*University of Mississippi, University, Mississippi 38677, USA*
[46]*Laboratoire René J. A. Lévesque, Université de Montréal, Montréal, QC, Canada H3C 3J7*
[47]*Mount Holyoke College, South Hadley, Massachusetts 01075, USA*
[48]*Dipartimento di Scienze Fisiche and INFN, Università di Napoli Federico II, I-80126, Napoli, Italy*
[49]*University of Notre Dame, Notre Dame, Indiana 46556, USA*
[50]*Oak Ridge National Laboratory, Oak Ridge, Tennessee 37831, USA*
[51]*The Ohio State University, 174 West 18th Avenue, Columbus, Ohio 43210, USA*
[52]*University of Oregon, Eugene, Oregon 97403, USA*
[53]*Dipartimento di Fisica and INFN, Università di Padova, I-35131 Padova, Italy*
[54]*Lab de Physique Nucléaire H. E., Universités Paris VI et VII, F-75252 Paris, France*
[55]*Dipartimento di Elettronica and INFN, Università di Pavia, I-27100 Pavia, Italy*
[56]*University of Pennsylvania, Philadelphia, Pennsylvania 19104, USA*
[57]*Scuola Normale Superiore and INFN, Università di Pisa, I-56010 Pisa, Italy*
[58]*Prairie View A&M University, Prairie View, Texas 77446, USA*
[59]*Princeton University, Princeton, New Jersey 08544, USA*
[60]*Dipartimento di Fisica and INFN, Università di Roma La Sapienza, I-00185 Roma, Italy*
[61]*Universität Rostock, D-18051 Rostock, Germany*
[62]*Rutherford Appleton Laboratory, Chilton, Didcot, Oxon OX11 0QX, United Kingdom*
[63]*DAPNIA, Commissariat à l'Energie Atomique/Saclay, F-91191 Gif-sur-Yvette, France*
[64]*University of South Carolina, Columbia, South Carolina 29208, USA*
[65]*Stanford Linear Accelerator Center, Stanford, California 94309, USA*
[66]*Stanford University, Stanford, California 94305-4060, USA*
[67]*University of Tennessee, Knoxville, Tennessee 37996, USA*
[68]*University of Texas at Dallas, Richardson, Texas 75083, USA*
[69]*Dipartimento di Fisica Sperimentale and INFN, Università di Torino, I-10125 Torino, Italy*
[70]*Dipartimento di Fisica and INFN, Università di Trieste, I-34127 Trieste, Italy*
[71]*TRIUMF, Vancouver, BC, Canada V6T 2A3*
[72]*Vanderbilt University, Nashville, Tennessee 37235, USA*
[73]*University of Victoria, Victoria, BC, Canada V8W 3P6*
[74]*University of Wisconsin, Madison, Wisconsin 53706, USA*
[75]*Yale University, New Haven, Connecticut 06511, USA*

(Received 27 December 2002; published 6 May 2003)

We present a measurement of the branching fraction for the rare decays $B \to \rho e \nu$ and extract a value for the magnitude of V_{ub}, one of the smallest elements of the Cabibbo-Kobayashi-Maskawa quark-mixing matrix. The results are given for five different calculations of form factors used to parametrize the hadronic current in semileptonic decays. Using a sample of 55×10^6 $B\bar{B}$ meson pairs recorded with the *BABAR* detector at the PEP-II e^+e^- storage ring, we obtain $\mathcal{B}(B^0 \to \rho^- e^+ \nu) = (3.29 \pm 0.42 \pm 0.47 \pm 0.55) \times 10^{-4}$ and $|V_{ub}| = (3.64 \pm 0.22 \pm 0.25^{+0.39}_{-0.56}) \times 10^{-3}$, where the uncertainties are statistical, systematic, and theoretical, respectively.

DOI: 10.1103/PhysRevLett.90.181801 PACS numbers: 13.20.He, 12.15.Hh, 14.40.Nd

Exclusive $b \to u \ell \nu$ decays can be used to determine $|V_{ub}|$, one of the smallest and least well-determined elements of the Cabibbo-Kobayashi-Maskawa quark-mixing matrix [1]. The modes $B \to \rho e \nu$ have a comparatively large branching fraction, and a high fraction of events is found at large electron momenta. We determine both the branching fraction $\mathcal{B}(B \to \rho e \nu)$ and $|V_{ub}|$ using form factors, which describe the hadronic current in the decay, to extrapolate the decay rates to the full range of lepton energies and to normalize $\mathcal{B}$ to $|V_{ub}|$. Five different form-factor calculations are used, as given in Table I.

The data in this analysis were collected with the *BABAR* detector [7] at the PEP-II [8] asymmetric-energy e^+e^- storage ring. The integrated luminosity of the sample recorded on the $\Upsilon(4S)$ resonance in years 2000 and 2001 ("on resonance") is $50.5\ \mathrm{fb}^{-1}$, corresponding to 55.2×10^6 $B\bar{B}$ meson pairs. An additional $8.7\ \mathrm{fb}^{-1}$ of data were taken 40 MeV below the resonance ("off resonance"). *BABAR* is a detector optimized for the asymmetric beam configuration at PEP-II. Charged-particle momenta are measured in a tracking system consisting of a 5-layer, double-sided silicon vertex tracker (SVT) and a 40-layer drift chamber (DCH) filled with a mixture of helium and isobutane, both operating in a 1.5-T superconducting solenoid. The electromagnetic calorimeter (EMC) consists of 6580 CsI(Tl) crystals arranged in barrel and forward end cap subdetectors. Particle identification is performed by combining information from ionization measurements in the SVT and DCH, energy deposits in the EMC, and the angle and number of Cherenkov photons measured by the DIRC (detector of internally reflected Cherenkov light).

We select decays in the modes $B^+ \to \rho^0 e^+ \nu$, $B^0 \to \rho^- e^+ \nu$, $B^+ \to \omega e^+ \nu$, $B^+ \to \pi^0 e^+ \nu$, and $B^0 \to \pi^- e^+ \nu$, with $\rho^0 \to \pi^+\pi^-$, $\rho^- \to \pi^0\pi^-$, and $\omega \to \pi^0\pi^+\pi^-$. The inclusion of charge conjugate decays is implied throughout. The analysis is optimized for $B \to \rho e \nu$ decays, similar to that in Ref. [9]. Signal events are sometimes reconstructed in one of the four other modes; the π and ω modes are included in order to estimate this cross feed into the ρ modes. Throughout this paper, all variables are expressed in the $\Upsilon(4S)$ center-of-mass frame, except if stated otherwise. Two electron-energy regions are considered: $2.0 \leq E_e < 2.3$ GeV (*low* E_e) and $2.3 \leq E_e < 2.7$ GeV (*high* E_e). A large background to $b \to u e \nu$ decays comes from the more copious $b \to c e \nu$ decays. This background is kinematically suppressed in the high-E_e region and dominates in the low-E_e region. The low-E_e region provides the background normalization in the high-E_e region. The largest background in the high-E_e region is continuum $e^+e^- \to q\bar{q}$ events. The off-resonance data are used to estimate its size.

TABLE I. Form-factor calculations used in the determination of $\mathcal{B}(B \to \rho e \nu)$ and $|V_{ub}|$, predicted normalizations $\tilde{\Gamma}_{\mathrm{th}}$ [as defined later in Eq. (3)], and the fraction of events with electron energies greater than 2.3 GeV.

Form factors	$\tilde{\Gamma}_{\mathrm{th}}$ (ps^{-1})	Error (%)	$\frac{\Gamma(E_e > 2.3\ \mathrm{GeV})}{\Gamma}$	Ref.
ISGW2	14.2	± 50	0.36	[2]
Beyer/Melikhov	16.0	± 15	0.27	[3]
UKQCD	16.5	$+21, -14$	0.28	[4]
LCSR	16.9	± 32	0.24	[5]
Ligeti/Wise	19.4	± 29	0.32	[6]

Hadronic events are selected based on track and photon multiplicity and event topology. We use tracks originating from the interaction point with at least 12 hits in the DCH and a transverse momentum greater than $0.1\ \mathrm{GeV}/c$. Signals in the EMC with $E_{\mathrm{lab}} > 30$ MeV that are not associated with any track are considered as photons if the lateral moment of the shower energy distribution [10] is smaller than 0.8. We select events with at least five tracks, or with at least four tracks and at least five photons. We require the ratio H_2/H_0 of Fox-Wolfram moments [11] to be less than 0.4. This requirement keeps 85% of the $\rho e \nu$ signal; it rejects 55% of the non-$B\bar{B}$ events.

Electrons are identified with a likelihood estimator using information from the DCH, EMC, and DIRC subdetectors [12]. The selection efficiency is around 90%, with a pion misidentification rate of less than 0.1%. We reject electrons from J/ψ decays and from photon conversions.

Charged pion candidates are tracks not identified as kaons based on DIRC and dE/dx measurements. A π^0 is reconstructed from photon pairs with an invariant mass $120 < M_{\gamma\gamma} < 145\ \mathrm{MeV}/c^2$.

To reconstruct ρ^0 mesons, we combine two oppositely charged pions, and for $\rho^\pm$ a pion track and a π^0. To suppress combinatorial background we require that the pion with the higher momentum satisfies $p_\pi > 400\ \mathrm{MeV}/c$ and the other pion $p_\pi > 200\ \mathrm{MeV}/c$. For the ω, we combine two oppositely charged pions with a π^0. To suppress the combinatorial background we require $p_\pi > 100\ \mathrm{MeV}/c$ for each pion. In the mode $B \to \pi e \nu$ we require $p_\pi > 200\ \mathrm{MeV}/c$.

The missing momentum in the event is given by

$$\vec{p}_{\mathrm{miss}} = -\sum_{\mathrm{tracks}} \vec{p}_i - \sum_{\mathrm{photons}} \vec{p}_i, \tag{1}$$

where the sums are over all accepted tracks and photons. We require $|\cos\theta_{\mathrm{miss}}| < 0.9$, where θ_{miss} is the angle between $\vec{p}_{\mathrm{miss}}$ and the beam axis. This rejects events with missing high-momentum particles close to the beam axis. We also compare the direction of $\vec{p}_{\mathrm{miss}}$ with that of the neutrino inferred from $\vec{p}_\nu = \vec{p}_B - \vec{p}_Y$, where Y is the $\rho + e$, $\omega + e$, or $\pi + e$ system. The latter is known to within an azimuthal ambiguity about the B direction since only the magnitude of $\vec{p}_B$ is known. We use the smallest possible angle $\Delta\theta_{\min}$ between the two directions and require $\cos\Delta\theta_{\min} > 0.8$. Using the constraints $E_B = E_{\mathrm{beam}}$ and $p_\nu^2 = (p_B - p_Y)^2 = 0$, the angle between the B meson and the Y system is

$$\cos\theta_{BY} = \frac{2E_B E_Y - (M_B^2 + M_Y^2)c^4}{2|\vec{p}_B||\vec{p}_Y|c^2}. \tag{2}$$

Signal events fulfill $|\cos\theta_{BY}| \leq 1$; allowing for detector resolution we require $|\cos\theta_{BY}| < 1.1$. After all other selection criteria, this requirement rejects more than 60% of the $b \to ce\nu$ and approximately 68% of the remaining continuum backgrounds; it retains 98% of the signal.

To further reduce the continuum background, we use a neural net with 14 event-shape variables: the sum of track and photon energies in nine cones centered on the lepton momentum; the angle θ_{thrust} between the thrust axis of the Y system and the thrust axis of the rest of the event (the thrust axis is defined to be the direction that maximizes the sum of the longitudinal momenta of all particles); the angle $\theta_{\text{thrust},Y}$ between the thrust of the Y system and the beam axis; the angle $\theta_{\text{lept,rest}}$ between the direction of the lepton and the direction of the total momentum of all tracks except the Y system; the momentum of the track with the smallest opening angle with respect to the electron; $\sum_i \vec{p}_i \cdot \vec{n}_e / \sum_i |\vec{p}_i|$, where $\vec{n}_e$ is the direction of the electron and $\vec{p}_i$ are the momenta of all tracks except the electron. After all other selection criteria, the neural net condition removes more than 90% of the continuum events in the high-E_e region, while retaining approximately 60% of the signal events in each signal mode.

After all selections, there remain on average 3.4 candidates per event. We choose the one with a total momentum $|\vec{p}_Y + \vec{p}_{\text{miss}}|$ closest to the B-meson momentum $|\vec{p}_B|$. The probability of making the right choice for the signal modes is approximately 85%.

The total efficiency in the high-E_e region is 12.0% (9.5%) for the mode $B^+ \to \rho^0 e^+ \nu$ ($B^0 \to \rho^- e^+ \nu$) in the ISGW2 model; it is 4.2% (3.3%), when relating the accepted events in the high-E_e region to events with all electron energies.

We perform a binned maximum-likelihood fit to the two-dimensional distribution ($M_{\pi\pi(\pi)}$, ΔE), where $M_{\pi\pi(\pi)}$ is the invariant mass of the ρ (ω) meson and ΔE is the difference between the reconstructed and the expected B-meson energy, $\Delta E \equiv E_{\text{hadron}} + E_e + |\vec{p}_{\text{miss}}|c - E_{\text{beam}}$. The fit is performed simultaneously for the five signal modes in the two E_e ranges. For the $B \to \rho e \nu$ modes, the data are divided into 10×10 bins over the ($M_{\pi\pi}$, ΔE) region $0.25 \le M_{\pi\pi} \le 2.00\ \text{GeV}/c^2$ and $|\Delta E| \le 2$ GeV. For the ω channel, we use five bins in the range $702 \le M_{\pi\pi\pi} \le 862\ \text{MeV}/c^2$ and ten bins in $|\Delta E| \le 2$ GeV. For the modes $B \to \pi e \nu$, only ΔE is used as a fit variable, also with ten bins.

In the fit, the likelihood is calculated as a product of probability distributions for each of the five signal modes, for other $b \to ue\nu$ decays, for $b \to ce\nu$ decays, for continuum events, and for a small contribution due to misidentified electrons. Shapes and normalizations of the continuum background and misidentified electrons are extracted from the data. For all other contributions, Monte Carlo (MC) simulation provides the shapes of the distributions. The decays $B \to D^{(*)} e \nu$ are simulated using a model based on heavy quark effective theory [13]. The modes $B \to D^{(*)} \pi e \nu$ are simulated according to the Goity-Roberts model [14]. The resonances $b \to ue\nu$ heavier than ρ and ω are implemented according to the ISGW2 model [2]. Nonresonant $b \to ue\nu$ modes are described by the model of De Fazio and Neubert [15].

The fit has nine free parameters: $\mathcal{B}(B^0 \to \rho^- e^+ \nu)$, $\mathcal{B}(B^0 \to \pi^- e^+ \nu)$, the normalization of the $b \to ue\nu$ background in the two electron-energy ranges (two parameters), and the normalization of the $b \to ce\nu$ background (five parameters, one for each mode). The rates of the ρ^0, ω, and π^0 channels are constrained by the isospin and quark model relations $\Gamma(B^0 \to \rho^- e^+ \nu) = 2\Gamma(B^+ \to \rho^0 e^+ \nu)$, $\Gamma(B^+ \to \rho^0 e^+ \nu) = \Gamma(B^+ \to \omega e^+ \nu)$, and $\Gamma(B^0 \to \pi^- e^+ \nu) = 2\Gamma(B^+ \to \pi^0 e^+ \nu)$. The maximum-likelihood fit takes into account the statistical uncertainties in the on- and off-resonance data and in the probability distributions extracted from MC simulations [16].

Projections of the data and fit results for $B^0 \to \rho^- e^+ \nu$ are shown in Fig. 1 for the ISGW2 model. A continuum-background contribution of 917 ± 73 events in high E_e and 1928 ± 106 in low E_e has been subtracted. Good agreement between data and the fit result is seen in each of these figures. The fits for the other form-factor calculations show the same level of agreement. The fit

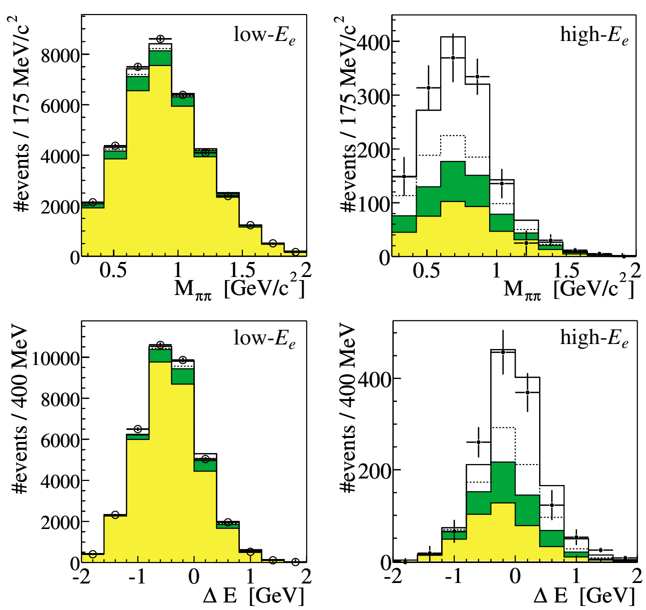

FIG. 1 (color online). Continuum-subtracted data distributions (points with error bars) and fit projections (histograms) for $M_{\pi\pi}$ (top plots) and ΔE (bottom plots) for the $B^0 \to \rho^- e^+ \nu$ channel in the low-E_e (left plots) and high-E_e regions (right plots). The fit results are shown for the ISGW2 model. The histograms correspond to the true and cross feed components of the signal (open histogram, above and below the dashed line, respectively), the background from other $b \to ue\nu$ decays (dark shaded region), and $b \to ce\nu$ and other backgrounds (light shaded region).

quality has been checked with a χ^2 test, where bins in sparsely populated regions have been combined before the χ^2 calculation. We obtain $\chi^2 = 91$ for 93 degrees of freedom for ISGW2, and similarly good fit quality for the other form-factor calculations. The signal yields extracted from the maximum-likelihood fit in the high-E_e region are 321 ± 40 $B^+ \to \rho^0 e^+ \nu$ events and 505 ± 63 $B^0 \to \rho^- e^+ \nu$ events. The resulting branching fractions $\mathcal{B}(B^0 \to \rho^- e^+ \nu)$ are shown in Fig. 2. The five fit parameters describing the $b \to c e \nu$ backgrounds agree well with the known branching fractions [17] for $B \to D e \nu$, $B \to D^* e \nu$, and $B \to D^{(*)}(\pi) e \nu$. The two parameters describing the size of the background from other $b \to u e \nu$ decays agree within 1.5σ with the predictions of the MC simulation. The ISGW2 result for the π modes is $\mathcal{B}(B^0 \to \pi^- e^+ \nu) = [1.86 \pm 0.56(\text{stat})] \times 10^{-4}$ in agreement with a previous measurement [18].

A summary of all considered systematic uncertainties on $\mathcal{B}(B \to \rho e \nu)$ is given in Table II. The relative systematic errors are the same for all five form-factor calculations. The total systematic uncertainty is the quadratic sum of all individual ones. Note that the statistical uncertainties in Fig. 2 already include the statistical uncertainty in the MC predictions. The largest single contribution to the systematic error arises from the uncertainty in the shape of the $b \to u e \nu$ background from events other than the signal modes. The fraction of $b \to u e \nu$ background events that are nonresonant is varied from 0 to 2/3 to estimate this uncertainty. The composition of the resonant component of other $b \to u e \nu$ decays has been varied by changing the branching fractions for individual resonances by $\pm 50\%$, while keeping the total rate constant. The branching fractions for $B \to D^{(*)} e \nu$ modes have been varied by $\pm 10\%$, and $\pm 40\%$ for other D modes. Possible violations of the isospin and quark model constraints are estimated in Ref. [19] to be smaller than 3%, leading to $\delta\mathcal{B}_\rho/\mathcal{B}_\rho < 1\%$. Several fits were performed: fitting without the ω mode, without the π mode [fixing $\mathcal{B}(B \to \pi e \nu)$ [17]], without the low-E_e region, and with different binning. We assign a systematic uncertainty for the fit method as half the largest resulting changes of the fit result. We have also varied the most important selection requirements and find that the changes in $\mathcal{B}(B \to \rho e \nu)$ are consistent with statistical variations as determined by a MC simulation.

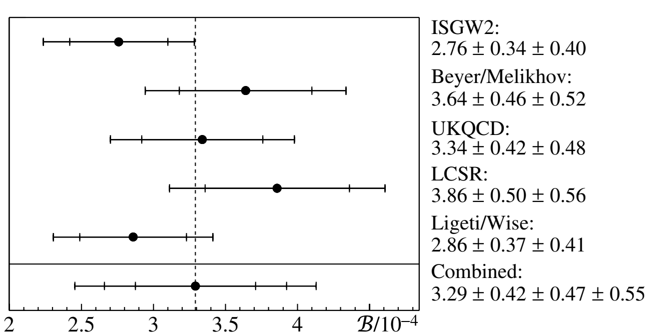

FIG. 2. The branching fraction $\mathcal{B}(B^0 \to \rho^- e^+ \nu)/10^{-4}$ results using five different form-factors calculations. The uncertainties shown are statistical, systematic, and (for the combined result) theoretical, successively added in quadrature. The combined result is the unweighted mean of the five form-factor results.

A value of $|V_{ub}|$ is determined by the relation

$$|V_{ub}| = \sqrt{\mathcal{B}(B^0 \to \rho^- e^+ \nu)/(\tilde{\Gamma}_{\text{th}} \tau_{B^0})}, \tag{3}$$

where $\tilde{\Gamma}_{\text{th}}$ is the predicted form-factor normalization as given in Table I. The branching fractions are used separately for each form-factor calculation, as shown in Fig. 2. We use $\tau_{B^0} = 1.542 \pm 0.016$ ps [17] for the B^0 lifetime. The results for $|V_{ub}|$ are shown in Fig. 3. The combined result is the weighted average of the five form-factor results, where the weight is obtained from the theoretical uncertainty of each. The estimated theoretical uncertainty on the combined result covers half of the full range of theoretical error bars; see Fig. 3. A more recent form-factor calculation [20] falls in the range of the other calculations.

In conclusion, we have measured the branching fraction $\mathcal{B}(B^0 \to \rho^- e^+ \nu) = (3.29 \pm 0.42 \pm 0.47 \pm 0.55) \times 10^{-4}$ using isospin constraints and extrapolating to all electron energies according to five different form-factor calculations. The errors given are statistical, systematic, and theoretical, in the order shown. The value of $|V_{ub}|$ determined by the same form-factor calculations is $|V_{ub}| = (3.64 \pm 0.22 \pm 0.25^{+0.39}_{-0.56}) \times 10^{-3}$. Our results are slightly higher (22% for $\mathcal{B}$ and 13% for $|V_{ub}|$) than a previous $B \to \rho e \nu$ result from CLEO [9], but agree within statistical errors.

TABLE II. Summary of all contributions to the systematic uncertainty on the branching fraction $\mathcal{B}(B \to \rho e \nu)$.

Contribution	$\delta\mathcal{B}_\rho/\mathcal{B}_\rho$ (%)
Tracking efficiency	± 5
Tracking resolution	± 1
π^0 efficiency	± 5
π^0 energy scale	± 3
$b \to c e \nu$ background composition	$+1.4, -1.7$
Resonant $b \to u e \nu$ background composition	$+6, -4$
Nonresonant $b \to u e \nu$ background	± 9
B lifetime	± 1
Number of $B\bar{B}$ pairs	± 1.6
Misidentified electrons	$< \pm 1$
Electron efficiency	± 2
$\mathcal{B}[\Upsilon(4S) \to B^+ B^-]/\mathcal{B}[\Upsilon(4S) \to B^0 \bar{B}^0]$	$< \pm 1$
Isospin and quark model symmetries	$< \pm 1$
Fit method	$+4, -6$
Total systematic uncertainty	± 14.4

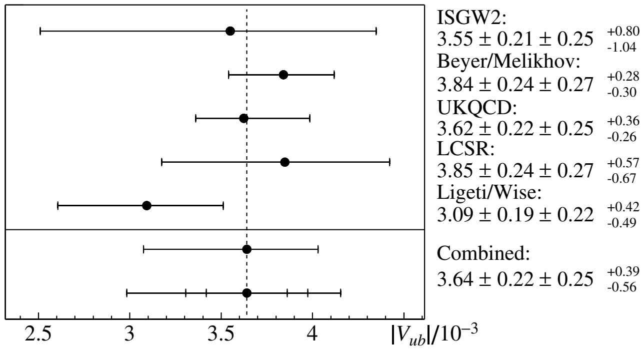

FIG. 3. $|V_{ub}|/10^{-3}$ determined using five different form-factor calculations. Only theoretical error bars are shown. The combined result is also shown at the bottom with statistical, systematic, and theoretical uncertainties successively added in quadrature.

We are grateful for the excellent luminosity and machine conditions provided by our PEP-II colleagues, and for the substantial dedicated effort from the computing organizations that support *BABAR*. The collaborating institutions wish to thank SLAC for its support and kind hospitality. This work is supported by DOE and NSF (U.S.A.), NSERC (Canada), IHEP (China), CEA and CNRS-IN2P3 (France), BMBF and DFG (Germany), INFN (Italy), NFR (Norway), MIST (Russia), and PPARC (United Kingdom). Individuals have received support from the A. P. Sloan Foundation, Research Corporation, and Alexander von Humboldt Foundation.

*Also with Università di Perugia, Perugia, Italy.
†Also with Università della Basilicata, Potenza, Italy.

[1] N. Cabibbo, Phys. Rev. Lett. **10**, 531 (1963); M. Kobayashi and T. Maskawa, Prog. Theor. Phys. **49**, 652 (1973).
[2] D. Scora and N. Isgur, Phys. Rev. D **52**, 2783 (1995).
[3] M. Beyer and D. Melikhov, Phys. Lett. B **436**, 344 (1998).
[4] L. Del Debbio *et al.*, Phys. Lett. B **416**, 392 (1998).
[5] P. Ball and V. M. Braun, Phys. Rev. D **58**, 094016 (1998).
[6] Z. Ligeti and M. B. Wise, Phys. Rev. D **53**, 4937 (1996).
[7] *BABAR* Collaboration, B. Aubert *et al.*, Nucl. Instrum. Methods Phys. Res., Sect. A **479**, 1 (2002).
[8] PEP-II Conceptual Design Report Report No. SLAC-PUB-418, LBL-5379, 1993.
[9] CLEO Collaboration, B. H. Behrens *et al.*, Phys. Rev. D **61**, 052001 (2000).
[10] A. Drescher *et al.*, Nucl. Instrum. Methods Phys. Res., Sect. A **237**, 464 (1985).
[11] G. C. Fox and S. Wolfram, Nucl. Phys. **B149**, 413 (1979).
[12] *BABAR* Collaboration, B. Aubert *et al.*, hep-ex/0208018, SLAC Report No. SLAC-PUB-9306.
[13] I. I. Bigi *et al.*, Annu. Rev. Nucl. Part. Sci. **47**, 591 (1997).
[14] J. L. Goity and W. Roberts, Phys. Rev. D **51**, 3459 (1995).
[15] F. De Fazio and M. Neubert, J. High Energy Phys. 9906 (1999) 017.
[16] R. J. Barlow and C. Beeston, Comput. Phys. Commun. **77**, 219 (1993).
[17] Particle Data Group, K. Hagiwara *et al.*, Phys. Rev. D **66**, 010001 (2002).
[18] J. P. Alexander *et al.*, Phys. Rev. Lett. **77**, 5000 (1996).
[19] D. J. Lange, Ph.D. thesis, UC Santa Barbara, 1999.
[20] A. Abada *et al.*, hep-lat/0209116.